Recognizing multiple kinds of ions specifically by ultrathin polymeric membranes with aligned angstrom pores for energy-efficient lithium extraction

Danying Zhao[1#], Wei Jiang[1, 2#], Jiale Zhou[2], Yan Ye[2], Yu Zhang[1], Zhenhua Jiang[1]，Lei Jiang[2]，Ke Zhou[3], Yahong Zhou[2*], and Yunhe Zhang[1*]*

[1]College of Chemistry, Jilin University, Changchun, P. R. China. [2]CAS Key Laboratory of Bio-inspired Materials and Interfacial Science, Technical Institute of Physics and Chemistry, Beijing, China. [3]College of Energy, Soochow Institute for Energy and Materials InnovationS (SIEMIS), Jiangsu Provincial Key Laboratory for Advanced Carbon Materials and Wearable Energy Technologies, Soochow University, Suzhou, China.

[#]These authors contributed equally: Danying Zhao, Wei Jiang.

E-mail: zhangyunhe@jlu.edu.cn; zhouyh@mail.ipc.ac.cn; zhouke@suda.edu.cn

1. Chemicals and Materials

Diallyl bisphenol A (DBA), 4,4'-dihydroxybiphenyl (DBP), and 4-fluorophenylsulfone (DPS) were procured from Energy Chemical. 5,10,15,20-Tetrakis (4-aminophenyl) porphyrin (TAPP), 3-chloroperoxybenzoic acid (mCPBA), and dimethylacetamide (DMAc) were sourced from Aladdin. Lithium chloride (LiCl), magnesium chloride ($MgCl_2$), calcium chloride ($CaCl_2$), copper (II) chloride dihydrate ($CuCl_2 \cdot 2H_2O$), ferric chloride ($FeCl_3$), aluminum chloride ($AlCl_3$), and potassium carbonate (K_2CO_3) were obtained from Sinopharm. Toluene and ethanol (EtOH) were purchased from Beijing Chemical Works. Cellulose acetate membranes were acquired from Shanghai Xin Ya Purification Equipment Co., Ltd. All chemicals were used without further purification.

2. Synthesis of PAES

Poly (aryl ether sulfone) containing acrylic side groups was synthesized via nucleophilic polycondensation, following the procedure reported in the literature. DBA, DBP, DPS, anhydrous K_2CO_3, DMAc, and toluene were introduced into a three-necked flask under a nitrogen atmosphere and dissolved. The mixture was refluxed at 135 °C for 2.5 hours to facilitate dehydration, where toluene removed water from the system. Post-dehydration, the excess toluene was evaporated by gradually heating the mixture to 165 °C. After complete toluene evaporation, the reaction was allowed to proceed for an additional 3 hours until the solution became viscous. The viscous solution was discharged into acidic deionized water while still hot, yielding white polymer strips. These strips were left to stand overnight, then pulverized into polymer particles using a high-speed grinder. The resulting polymer was washed three times with boiling deionized water and ethanol to obtain the polymer PAES.

3. Synthesis of PAES-PO

To synthesize PAES- PO, 3 g of PAES polymer was dissolved in 30 mL of DCM with continuous stirring at room temperature, followed by cooling in an ice-water bath. In a separate beaker, 4.36 g of mCPBA was dissolved in 40 mL of DCM, cooled, and then slowly added dropwise to the polymer solution. The reaction was maintained in the ice-water bath for 2 hours, followed by gradual warming to room temperature for a further 30 hours. As the reaction progressed, the initially transparent light-yellow solution

deepened in color. The reaction mixture was then poured into 400 mL of anhydrous ethanol, allowed to stand, and the white fibrous polymer was filtered out. The polymer was redissolved in 20 mL of DCM, precipitated again in ethanol, and dried to yield polyarylether sulfone containing epoxy side groups.

4. Synthesis of PAES-TAPP

For the synthesis of PAES-TAPP, 500 mg of PAES-PO polymer was dissolved in a suitable amount of DMAc. Subsequently, 147.5 mg of tetraamino porphyrin was added, and the reaction was conducted at 100 °C for 2 hours. The mixture was precipitated in ethanol, and the solid obtained was dissolved in a small amount of DCM solvent. The solution was then precipitated again in ethanol to yield the final product.

5. Fabrication of Membranes

Casting Method: A solution of the polymer in DMAc was cast onto a glass plate, and the solvent was evaporated in a blast oven, forming a polymer membrane approximately 200 nm thick.

Water Surface Spreading Method: A polymer solution in DCM at a concentration of 20 mg/mL was spread onto a water surface. As the solvent evaporated, a polymer membrane less than 20 nm thick was formed.

6. Measurement Techniques

Nuclear Magnetic Resonance (NMR): ^{1}H NMR spectra were recorded using a Bruker AVANCE III spectrometer (400 MHz) with $CDCl_3$ as the solvent.

Fourier Transform Infrared Spectroscopy (FT-IR): FT-IR spectra were recorded on a Varian Excalibur 3100 spectrometer.

Powder X-ray Diffraction (PXRD): PXRD patterns were obtained using a Rigaku Smart Lab diffractometer with Cu Kα radiation (λ = 1.5406 Å), scanning in the 2θ range of 4–50° at a step size of 0.05° at room temperature.

Scanning Electron Microscopy (SEM): Membranes were gold-coated before examination. SEM imaging was performed using a Hitachi S-4800 microscope at 5 kV.

Atomic Force Microscopy (AFM): Thin membrane samples were mounted on wafers for AFM imaging, which was conducted using a Bruker Fastscan instrument in phase mode.

Transmission Electron Microscopy (TEM): Membrane samples were sonicated in anhydrous ethanol for 1 hour, then the upper solution was dropped onto an ultrathin carbon film, dried, and analyzed. TEM images were captured using a JEM 2100 at an accelerating voltage of 80 kV.

7. Electrical Measurements: Electrical measurements were conducted using a Keithley 6487 semiconductor picoammeter with a pair of custom-made Ag/AgCl electrodes. Membranes were clamped between two chambers, with an effective test area of approximately 2.8×10^{-17} m². Membranes were immersed in chloride solution of six metal cations respectively (Fe^{3+}, Al^{3+}, Mg^{2+}, Ca^{2+}, Cu^{2+}, Li^{+}).

Ion Separation Performance under Electric-Driven Gradient: The membrane's ion separation performance was evaluated under an applied step voltage (current reached 10^{-9} A). Initially, the membrane was immersed in salt solutions of equal concentration on both sides, and a voltage of 200 mV was applied to ensure current flow, confirming proper device setup. The system was then rinsed with deionized water to remove any residual ions. Finally, the current response was measured as the applied step voltage was gradually increased. When the current reaches 1×10^{-10} A, the membrane is considered to have ions passing through.

8. Density functional theory (DFT) calculation. *Ab-initio* Born-Oppenheimer MD simulation is performed to study the transport of proton using the CP2K package[1]. We use a hybrid Gaussian and plane waves (GPW) scheme where the electronic density is expanded in the form of plane waves with a cutoff of 500 Ry[2]. The molecularly optimized Gaussian basis sets are used (mDZVP)[3]. Goedecker-Teter-Hutter (GTH) pseudopotentials are used to treat the core electrons[4]. PBE+D3 are used for the exchange and correlation functional[5,6]. For the simulation of ion binding with nanopore, a cubic cell with one porphyrin molecule and 79 water molecules are used. Single ion is solved in the water box. The simulation box is relaxed at zero pressure by the reactive force-field (ReaxFF) interatomic potential[7] for 2 ns using NPT assemble performed by the large-scale atomic/molecular massively parallel simulator (LAMMPS)[8] before running AIMD.   Periodic boundary conditions are applied in all directions. The PMF

is calculated using the umbrella sampling (US) method[9]. The reaction coordinate (d) is defined as the distance between the ion's position and the geometric center of the porphyrin ring. The d is restrained by a harmonic spring at certain position (see the position of US window and spring constant in **Table 3**). Each US window runs in an individual simulation of 100 ps that the first 10 ps is discard for data analysis. The PMFs are generated by recombining individually biased distributions using the umbrella integration method[10]. Simulations are carried out using the Nose-Hoover thermostat (NVT assemble) with a damping constant of 100 fs. To reproduce the structure of water at ambient conditions (298 K, 1 atm), the higher temperature of 390 K was used[11]. The time step to integrate the Newtonian equations is 1.0 fs.
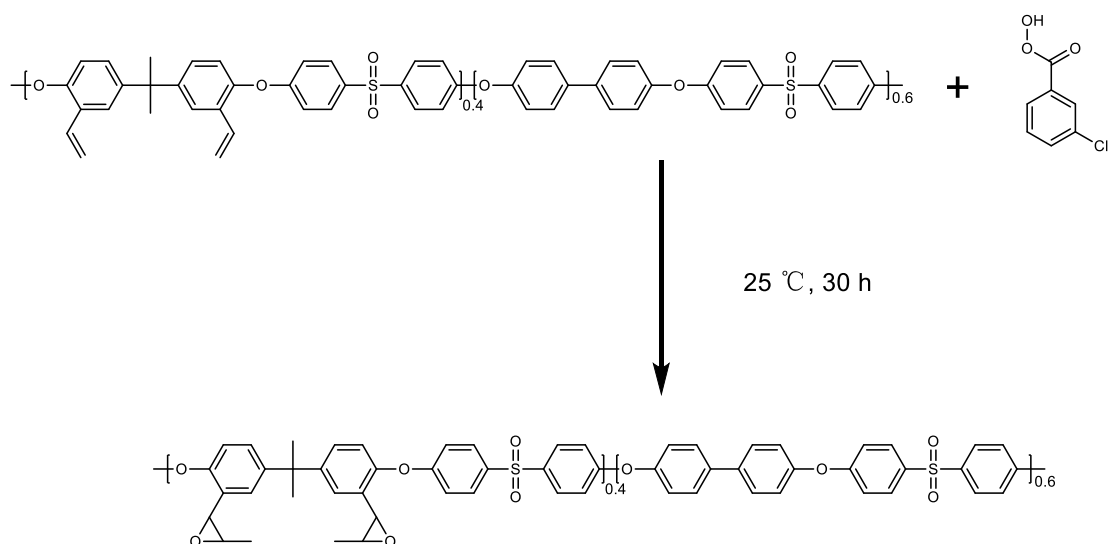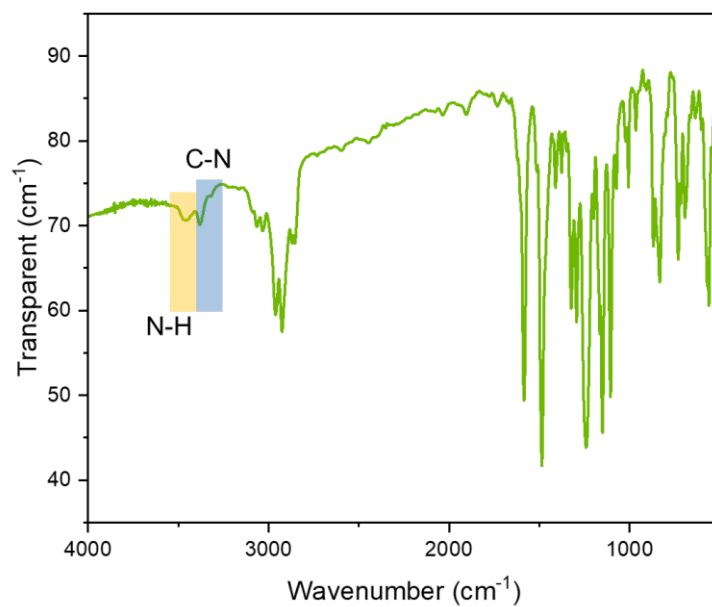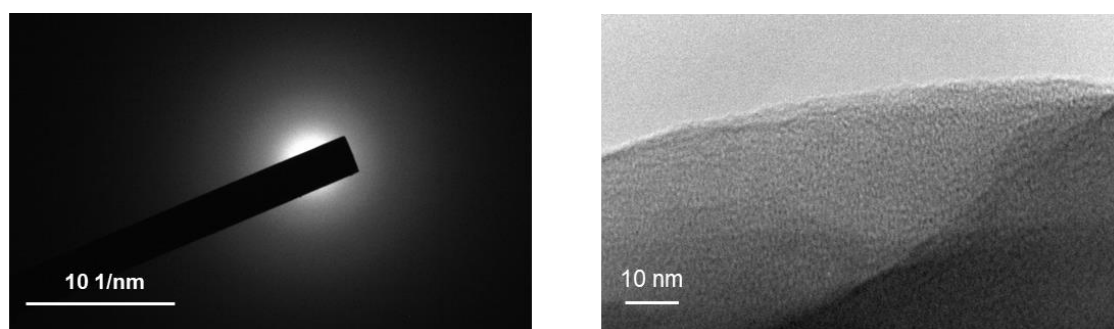
Supplementary Figure 1 Synthetic route of PAES-PO.
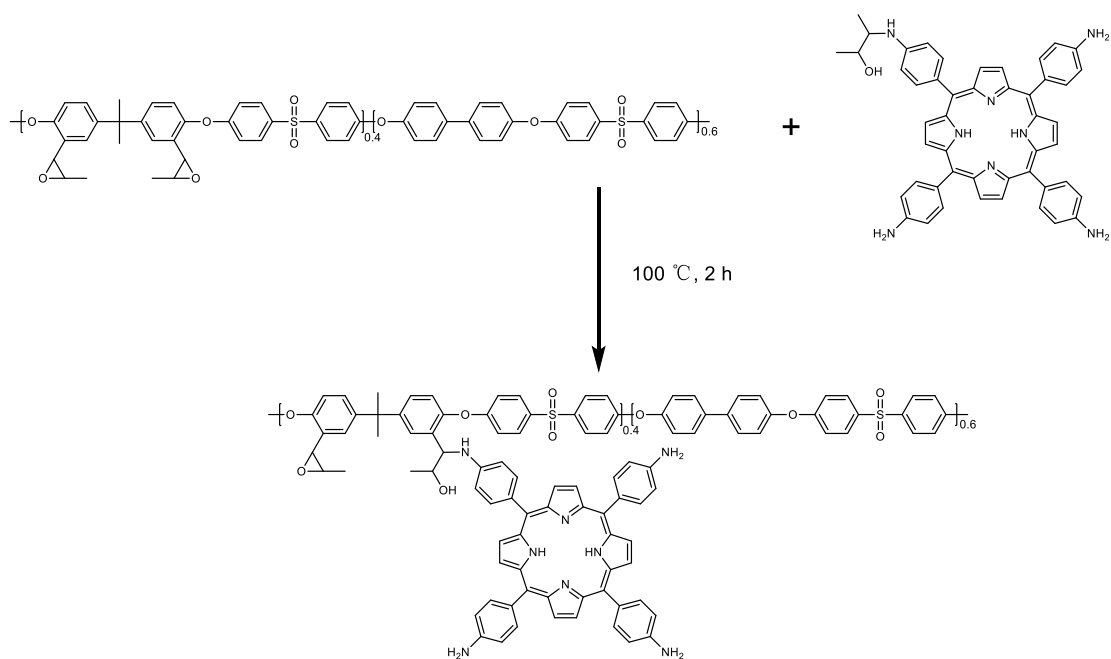
Supplementary Figure 2 Synthetic route of PAES-TAPP.

Supplementary Figure 3 1H NMR spectrum of PAES-PO in CDCl₃.

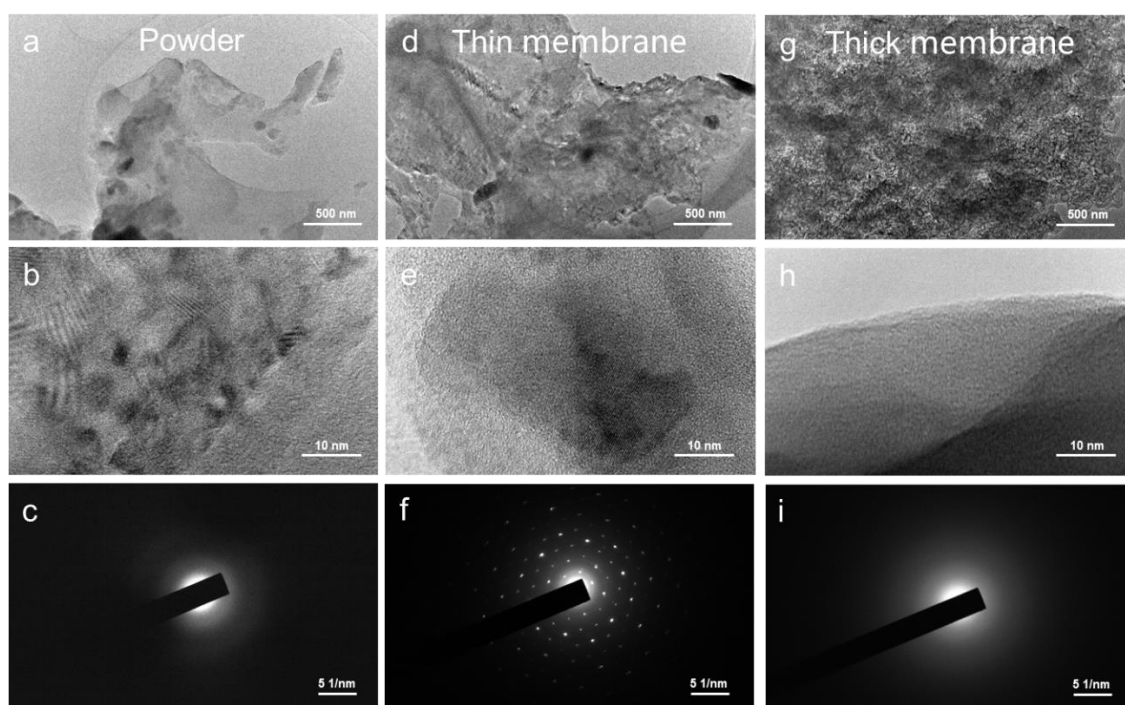**Supplementary Figure 4** 1H NMR spectrum of PAES-TAPP in CDCl₃.

**Supplementary Figure 5** FITR spectrum of PAES-TAPP.

Supplementary Figure 6 TEM image and SAED of PAES by surface superspreading strategy.

Supplementary Figure 7 TEM image and SAED of PAES-TAPP by surface superspreading strategy. a-c) Powder of PAES-TAPP. d-f) ultrathin membrane of PAES-TAPP. g-i) Thick membrane of PAES-TAPP.
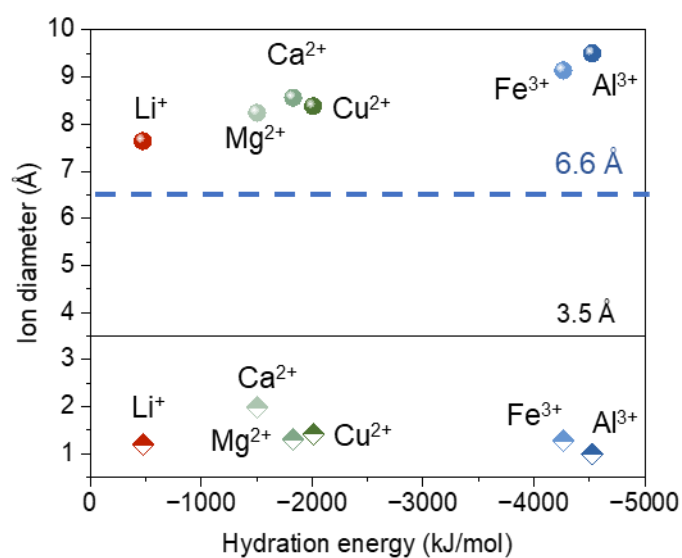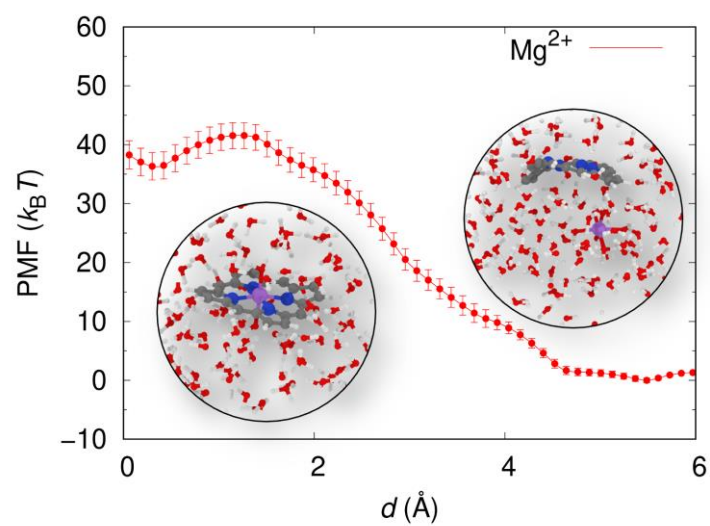

Supplementary Figure 8 The hydrated ion radius, crystal ion radius and dehydration energy of various ions. Dehydration energy is not the main energy factor that determines the passage of ions through the membrane.
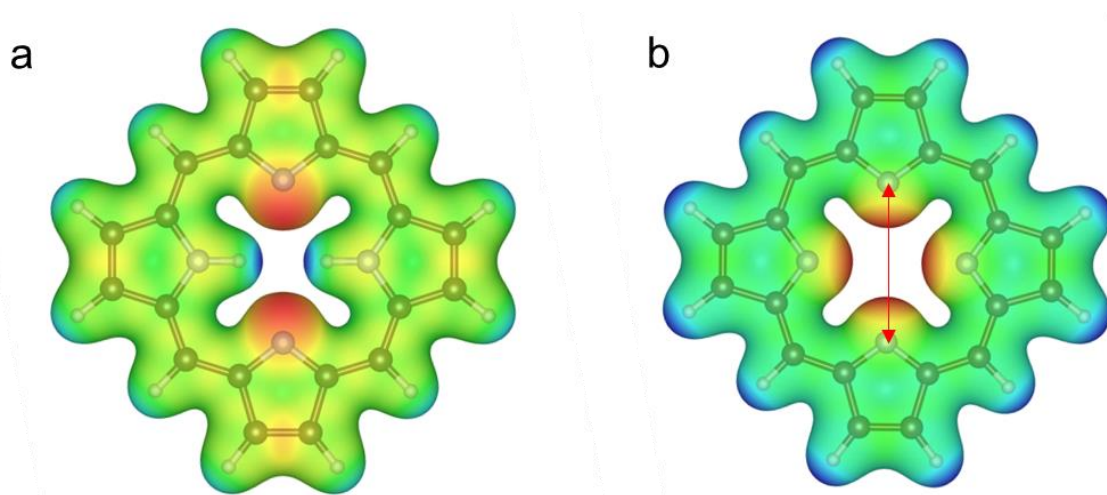
Supplementary Figure 9 The Geometry of Porphyrin Ring. a) The Geometry of Porphyrin Ring with H atoms on N atoms. b) The Geometry of Porphyrin Ring without H atoms on N atoms. The pore size of porphyrin is extremely tiny, the space for the binding ions is 4.18-0.75*2≈2.5 Å.
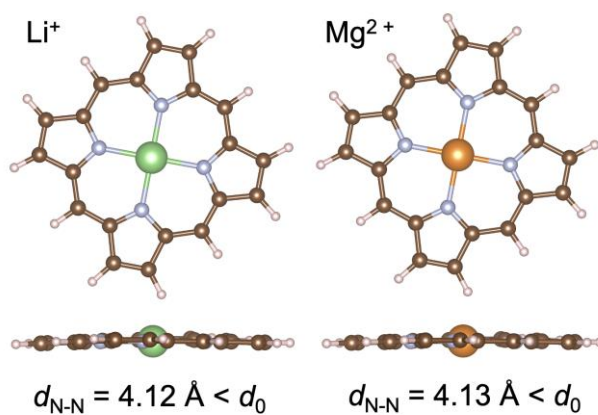
Supplementary Figure 10 The optimized structure of ion binding on porphyrin molecule. The distance of N-N atom (d_{N-N}) is indicated on the figure. Here, d_0 is the d_{N-N} without ions (4.18 Å).

Supplementary Figure 11 The potential of mean force (PMF) for Mg^{2+}. The inset is the snapshot for $d = 0$ Å and 6 Å.

Ions	Crystal ionic diameter (Å)	Hydrated ionic diameter (Å)	Hydration energy (kJ/mol)[2]
Li^+	0.90	7.64	489
Mg^{2+}	0.86	8.56	1837
Ca^{2+}	1.14	8.24	1527
Cu^{2+}	0.87	8.38	2028
Al^{3+}	0.68	9.5	4554
Fe^{3+}	0.69	9.14	4296

Supplementary Table 1 The hydrated ion radius, crystal ion radius and dehydration energy of various ions.

Ref	Li$^+$ concentration (M)	Energy consumption (Wh·g$_{Li}^{-1}$)	Voltage (V)
30	2.43E-05	2.48	0.6
	0.143	3.68	0.6
31	0.005	19.31	5
	0.01	19.31	5
33	0.00357	7.06	1.8
	0.0169	7	1.8
32	0.05	115.26	1.5
	0.05	541.13	7
34	5.00E-06	33.25	1.5
	5.00E-06	9.05	1.5
	5.00E-06	15.22	1.5
	5.00E-06	121.21	2
35	0.1	96.53	5
36	3.00E-05	26.7	3.25
	3.00E-05	12.56	3.25
38	0.1	19.33	5
	0.1	19.33	5
	0.1	19.33	5
	0.1	20.54	5
	0.03	1.09	0.25
37	0.03	2.27	0.5
	0.03	4.58	0.7
This work	1.00E-04	1.10E-04	0.4
	0.001	1.40E-04	0.25
	0.01	1.86E-04	0.003

Supplementary Table 2 Performance data of other direct lithium extraction works shown in Fig 4c.

Ions	Position of windows (Å)	Force constant for harmonic spring (kj/mol/Å^2)
Li$^+$	0.0, 1.0, 2.0, 3.0, 4.0, 5.0, 6.0	100,100,100,100,50,50,50
Mg^{2+}	0.0, 1.0, 1.5, 2.0, 3.0, 4.0, 5.0, 6.0	100,100,100,100,100,100,100,100

Supplementary Table 3 The positions of windows and force constant for harmonic spring for the simulation of umbrella sampling.

References

1   Hutter, J., Iannuzzi, M., Schiffmann, F. & VandeVondele, J. cp2k: atomistic simulations of condensed matter systems. *Wires. Comput. Mol. Sci.* **4**, 15-25 (2014).

2   LIPPERT, B. G., PARRINELLO, J. H. & MICHELE. A hybrid Gaussian and plane wave density functional scheme. *Mol. Phys.* **92**, 477-488 (1997).

3   VandeVondele, J. & Hutter, J. Gaussian basis sets for accurate calculations on molecular systems in gas and condensed phases. *J. Chem. Phys.* **127**, 114105 (2007).

4   Goedecker, S., Teter, M. & Hutter, J. Separable dual-space Gaussian pseudopotentials. *Phys. Rev. B* **54**, 1703 (1996).

5   Perdew, J. P., Burke, K. & Ernzerhof, M. Generalized gradient approximation made simple. *Phys. Rev. Lett.* **77**, 3865 (1996).

6   Grimme, S., Antony, J., Ehrlich, S. & Krieg, H. A consistent and accurate ab initio parametrization of density functional dispersion correction (DFT-D) for the 94 elements H-Pu. *J. Chem. Phys.* **132**, 154104 (2010).

7   Zhang, W. & Van Duin, A. C. Improvement of the ReaxFF description for functionalized hydrocarbon/water weak interactions in the condensed phase. *J. Phys. Chem. B* **122**, 4083-4092 (2018).

8   Plimpton, S. Fast parallel algorithms for short-range molecular dynamics. *J. Comput. Phys.* **117**, 1-19 (1995).

9   Roux, B. The calculation of the potential of mean force using computer simulations. *Comput. Phys. Commun.* **91**, 275-282 (1995).

10   Kästner, J. & Thiel, W. Bridging the gap between thermodynamic integration and umbrella sampling provides a novel analysis method:"Umbrella integration". *J. Chem. Phys.* **123** (2005).

11   Zhou, K., Qian, C. & Liu, Y. Quantifying the structure of water and hydrated monovalent ions by density functional theory-based molecular dynamics. *J. Phys. Chem. C* **126**, 10471-10480 (2022).